Nanomechanical and Optical Studies on Polymeric Membranes

C. Charitidis, M. Gioti, S. Logothetidis*

Aristotle University of Thessaloniki, Department of Physics, GR-54124 Thessaloniki, Greece
E-mail: cchar@skiathos.physics.auth.gr

Summary: The nanomechanical properties of poly(ethylene terephthalate) (PET) membranes, were examined in light of nanoindentation experiments under conditions of maximum contact load in the range of 0.5-12 mN. Spectroscopic Ellipsometry (SE) from 1.5 to 6.5 eV (Vis–FUV range) was also applied to probe the dielectric function ($\varepsilon(\omega)$) of the industrially supplied membranes, as well as their geometrical structure. Mechanical stretching (uniaxial or biaxial) procedures are usually applied for the elongation of the polymeric membranes, their thickness reduction and enhancement of their mechanical and optical performance, causing a preferable orientation of the macromolecules close to the surface. Nanoindentation and SE testing have revealed the existence of a two-layer geometrical structure of the PET membranes, consisting of a thick amorphous PET layer and a thin crystalline-like PET overlayer, with increased hardness (elastic modulus). The analyses of the experimental dataprovides quantitative information on the formed overlayer, which is ascribed to the processing history of the membrane.

Keywords: hardness; indentation; mechanical properties; membranes; modulus; optical properties; PET

Introduction

In the last two decades, polymer research for a number of both low-tech and high-tech applications presents an increasing interest. Poly(ethylene terephthalate) (PET) is extensively used in the fabrication of high performance polarization optics due to its high anisotropy and a relatively wide transparent spectral window.[1] PET also demonstrates an excellent combination of properties, which are of high importance for packaging applications, such as easy processing, good mechanical properties, and reasonably low permeability to oxygen and carbon dioxide gases (barrier properties).[2-3] Crystallization, in particular cold-crystallization from the glassy state, is traditionally considered as one of the most practical and simple approaches to improve PET's mechanical and optical properties, and gas permeability.

 DOI: 10.1002/masy.200450122

Mechanical stretching (uniaxial or biaxial) is usually applied for the elongation of the polymeric membranes and their thickness reduction, and causes a preferable orientation of the macromolecules close to the surface. However, such procedures cannot be fully controlled concerning the achievable degree of ordering and the thickness of the formed ordered overlayer, which we will call crystalline layer.

The main scope of this work is the study of the nanomechnical and optical properties of PET, as a representative polymeric membrane and this is carried out using both nanoindentation technique for nanomechanical properties and Spectroscopic Ellipsometry (SE) as the principal characterization and analytical technique for the determination of the optical and electronic parameters and constants of the transparent polymeric membranes, which are close related to their nanomechanical properties and microstructure. The so far published works on this issue are SE studies in a narrow energy range at Vis-UV region, where the polymeric materials are more or less transparent and little and ambiguous information can be derived by their analysis concerning their optical and electronic properties.[4]

Surface and near-surface mechanical properties of thin films and coatings can be critical to their final performance. The rapidly expanding field of depth-sensing nanoindentation provides a quantitative method for mapping the mechanical properties, such as hardness (H) and elastic modulus (E), of the surface/near-surface region. Quantification is possible through the use of diamond indenters with well-defined tip geometry, combined with established models for determining the mechanical properties from the measured data. Nanoindentation techniques have been employed extensively to measure the nanomechanical properties of a wide range of hard coatings and surface-modified layers. However, the determination of the surface mechanical properties of polymeric materials with such techniques is relatively new. Despite the insights which microhardness testing has provided, far fewer studies of the nanoscale indentation of polymeric materials have been reported,[5-10] presumably due to the time-dependent mechanical behavior which complicates the interpretation of the results.

PET films have been subject to extensive characterization at the macroscale and less at the nanoscale,[9,11,12] and therefore is an ideal material to investigate the applicability of depth-sensing indentation to the mechanical characterization of polymeric materials at the nano/microscale.

In the indentation study, we investigate the effect of film processing history on the mechanical properties (hardness, modulus, indentation index) of the film. The relationships between the indentation response and the results of the Spectroscopic Ellipsometry measurements and analyses have been compared. We were interested to determine whether there was a direct correlation between the film hardness and its crystallinity.

Experimental Details

The examined PET membranes were industrially supplied samples of a thickness ~12 μm, which had been treated using mechanical biaxial stretching that is usually applied in industrial scale. This procedure resulted to the formation of a crystalline-like layer on top of the membrane of unknown thickness.

The Vis – FUV spectra were carried out by means of a Phase Modulated Ellipsometer (PME) of Jobin-Yvon/Horiba at an angle of incidence of 70°, over the range 190 – 830 nm. The unit is consisted by two photomultiplier detectors; one for the UV – Vis range (310 – 830 nm) and one for the FUV – UV range (190 – 310 nm). The light source was a proper Xe lamp 150 W, having high intensity at FUV, and the whole energy spectrum was acquired using a special designed monochromator. All the optical and polarized components of the system were suitable for the FUV.

The elastic properties of the films were conducted using a Nano Indenter XP system. The H and E of each of the films were measured with a Berkovich, three-sided pyramid diamond indenter with nominal angle of 65.3° between the tip axis and the faces of the triangular pyramid, which was forced into the specimen surface by using a coil and magnet assembly. The system has load (displacement) resolution of 50 nN (<0.01 nm). The position of the indenter is determined from a capacitance gage. The entire system, including the position of the specimen table, is computer-controlled. The isolation of the system includes the environmental isolation cabinet and the vibration isolation table in order to prevent it from thermal or acoustic disturbance during operation. Experiments were performed in a clean-air environment of ~45% relative humidity and 22(1)°C ambient temperature. The samples to be measured were placed into the cabinet for several hours prior to testing, in order to reach equilibrium with the thermal mass inside the cabinet. Prior to each indentation test, two indents in 100 nm depth were conducted in fused silica to evaluate the tip condition.

In conventional depth-sensing indentation testing, the stiffness of contact is determined through the unloading curve. This means that H and E are known at the points of unloading i.e., at specific depths. A recently developed technique, continuous stiffness measurement (CSM),[13] offers a significant improvement in nanoindentation testing. The CSM is accomplished by imposing a small, sinusoidally varying signal on top of a DC signal that drives the motion of the indenter. By analyzing the response of the system by means of a frequency specific amplifier data are obtained. This allows the measurement of contact stiffness at any point along the loading curve and not just at the point of unloading as in the conventional measurement. The CSM technique makes the continuous measurement of mechanical properties of materials possible in one sample experiment without the need for discrete unloading cycles, and with a time constant that is at least three orders of magnitude smaller than the time constant of the more conventional method of determining stiffness from the slope of an unloading curve. The measurements can be made at exceedingly small penetration depths. Thus, this technique is ideal for mechanical property measurements of nanometer-thick films. Furthermore, its small time constant makes it especially useful for measuring the properties of polymeric materials. In non uniform materials, such as graded materials and multilayers, the microstructure and mechanical properties change with indentation depth. Continuous measurements of mechanical properties of these materials during indentation are greatly needed.

In all CI and CSM depth-sensing tests a total of ten indents were averaged to determine the mean H and E values for statistical purposes, with a spacing of 50 μm. The shallowest data points are often outside the limits of the theoretical depth resolution. If spurious data points from extremely shallow depths are used, the area calculated from these data points can be either extremely small or extremely large. In order to exclude any such data from the H and E curves, a default value of 5 nm was given to the minimum contact depth.

Results and Discussion

For a thin transparent film grown on bulk substrate or in general for a transparent material (like PET membrane which is our case) the measured quantity by SE is the "pseudodielectric function" ($\langle\varepsilon(\omega)\rangle$) which carries information for the film thickness in addition to the dielectric response. A typical Vis – FUV spectra of $\langle\varepsilon(\omega)\rangle$ obtained for PET membrane is

illustrated in Fig. 1. The optical transparency of PET in the energy range 300 – 830 nm is evident through the interference fringes originated by the multiple reflections of light at the interfaces of the sample under study. So, in the Vis – UV zone there are no absorbance bands, but interference fringes of two kinds are distinguished: i) one with low number of oscillations per wavelength, and ii) others with high number of oscillations per wavelength. These two different types of modulations arised from the geometrical structure of the membranes. More specifically, the first interference fringes are due to a crystalline-like overlayer and the second fringes contain information on the total thickness of an amorphous membrane.

The energies where the two different kinds of the fringes are eliminated are strongly correlated to the amorphous or crystalline nature of the layers. Since the upper and thinner layer (PET overlayer) has a crystalline-like microstructure, it is expected to present a higher fundamental band gap comparing to its amorphous counterpart, which is the thick underlying layer of PET. The fringes attributed to the former are eliminated at ~ 300 nm, whereas the fringes attributed to the latter are diminished below the ~ 500 nm. The two characteristic features appeared in the UV – FUV region of the spectrum; below 275 nm, are due to the strong electronic absorption of the crystalline PET.

In order to fit the SE spectra deduced by PET films we applied the four-layer model: air/c-PET/a-PET/air in combination to Tauc-Lorentz (TL)[14,15] oscillator model for the description of the dielectric response of amorphous (1-TL) and crystalline (2-TL) PET layers. By applying a minimization fitting procedure we calculated the parameters of 1-TL and 2-TL as well as the thicknesses of a-PET and c-PET. The corresponding calculated $\langle\varepsilon(\omega)\rangle$ using the best-fit parameters has been also plotted in Fig. 1 for comparison (solid lines). The calculated bulk dielectric functions for the a-PET and the c-PET are presented in Fig. 2, together with a schematic description of the geometrical structure of the examined specimen in which the calculated thicknesses of the layers are presented. The $\varepsilon(\omega)$ of the a-PET is characterized by the lower $\varepsilon_1(\omega)$ values at the higher wavelength range, comparing to that of c-PET, and the broad peak corresponding to the total electronic absorption take place in a-PET, unlike to c-PET where the electronic transitions at different energies are well separated. Both of these characteristics and differences are expected between an amorphous material and its crystalline counterpart, and based on these the detection and the verification of the 2-layer structure of the studied PET membranes using SE becomes feasible.

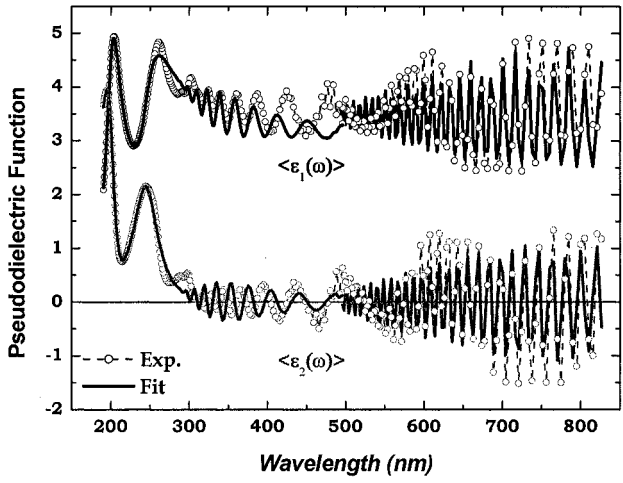

Figure 1. The experimental (symbols) and fitted (solid lines) <ε(ω)> of PET membrane in the Vis-FUV range, using 1-TL and 2-TL oscillators model in combination to 4-layer model.

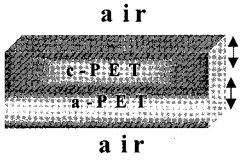

$d^{c\text{-}PET}$= 500 – 600 nm
$d^{a\text{-}PET}$ ~ 1000 nm

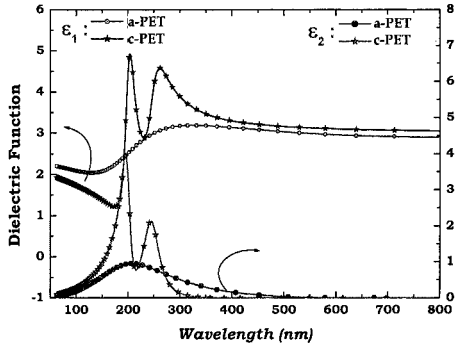

Figure 2. The calculated bulk ε(ω) for the PET and overlayer using the best-fit parameters. It is also shown the geometrical model of the blank PET film and the respective calculated thicknesses by SE.

A number of problems exist with the current application of nanoindentation techniques to polymeric materials using nanoindentation. In general, measurements of E tend to increase with decreasing penetration depth, often referred to as an indentation size effect. Thus, either

E(surface) > E(bulk) for a large number of materials, which seems unlikely, or these trends result from increased uncertainties for shallow depth indents that are likely due to tip defects near the apex and decreased signal-to-noise ratios at low load and displacement levels. For some studies, modulus values measured using nanoindentation has been compared to handbook or manufacturer values. However, such comparisons can often be misleading, because quoted values of E for many polymer systems can cover a large range due to potential variations in microstructure, semicrystalline morphology, anisotropy, molecular weight, crosslink density, etc. Thus, comparisons of modulus values are most appropriate for polymer samples with identical chemistry, molecular weight, and processing history.

In Fig. 3 a schematic load-unload cycle in PET film is shown. The creep occurring during the hold period at maximum load is indicated by an arrow.

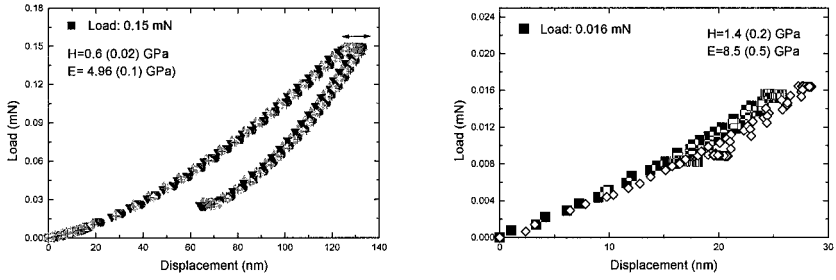

Figure 3. Evolution of the applied load vs. the penetration depth (Displacement) upon nanoindentation cycle, for maximum load 0.15 mN (a) and 0.016 mN (b).

Figure 4 shows the variation in hardness and modulus with contact depth, using the CSM option calculated from 10 indentations, covering the loading range 0.01–2.2 mN, into PET membrane surface. The loading rate was 0.05 mN/s and the dwell time 50 s in all the tests. Figure 4 shows a pronounced rise in hardness and modulus as the indentation depth decreases. Both H and E are increased in the surface/near surface region (1.5 and 8.5 GPa, respectively), while for higher contact depths, corresponding in the bulk of the PET membranes the H (E) values tend to decrease approaching the bulk H and E values (0.4 and 3.5 GPa, respectively). The bulk H and E values are in good agreement with measurements in the literature.[16]

The increases in hardness and modulus became more pronounced when indenting to less than 400 nm from the film surface. The near constant hardness above 400 nm is in agreement with the results of other researchers on PET films.[5, 9]

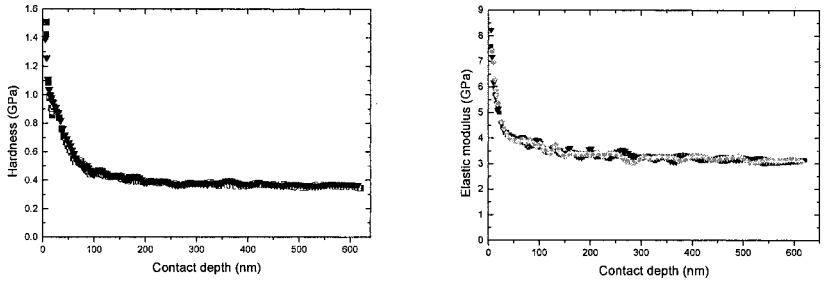

Figure 4. Hardness and Elastic Modulus vs. Contact depth (CSM).

In the Table I values of H and E measured using both CI and CSM at the surface/near surface of PET membranes are presented.

Table I. H & E values of PET membranes measured using CI and CSM techniques.

	H (GPa)	E (GPa)	H (GPa)	E (GPa)
	(Resulting Contact depth ~30 nm)		(Resulting Contact depth ~130 nm)	
CSM	1.5	8.5	0.48	3.8
CI	Maximum load: 0.016 mN		Maximum load: 0.15 mN	
	1.4	8.5	0.6	4.96

Comparing the results from the CI and CSM depth-sensing measurements (Figs. 3 & 4, and Table I) it seems that they are in good agreement. More specific, the H(E) values measured by CI, at a maximum load 0.016 mN are in excellent agreement with those measured by CSM. For a maximum load 0.15 mN and resulting penetration depth ~130 nm, H and E values measured by CI are increased (~20%) in comparison with those measured by CSM at a contact depth 130 nm.

In all the CI data reported in this paper, the loading data have been fitted to the power-law function: $P=\alpha\ h^n$, where P is the load, α, a material parameter and n, the index of the deformation (indentation index), to determine this depth offset.

The fit of the loading curve data to the function $P=\ a\ h^n$ is very good. Figure 5 shows a typical power-law fit to 0.018 and 1 mN indentation into the PET membrane; the fitted curve superimposes virtually exactly over the loading data. When a Berkovich indenter is used, the value of n is often very close to 2.[17,18] However, deviations from this are known to occur, particularly for polymers (e.g. due to strain-rate effects), and are discussed in more detail in the following.

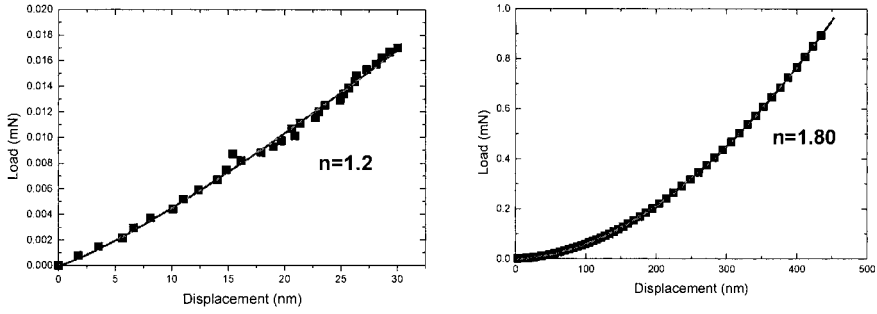

Figure 5. Typical loading behavior of PET membranes during nanoindentation in the load range 0.018-1 mN. The solid lines represent fitting of the load data using the equation P=a hn, n: indentation index in different Displacement of the indenter in PET membranes.

In Fig. 6 indentation index vs. Displacement of the indenter in PET is presented. Figure 6 reveals the existence of a near surface region of about 400 nm in thickness, where the indentation index rises from 1.2 to 1.80. For penetration depths above 400-450 nm, the indentation index is nearly stable (n=1.80).

It is interesting to speculate on whether the increase in hardness in surface/near to the surface is an indentation size effect, or represents a change in the mechanical properties of the near-surface region due to enhanced crystallinity. On polymers which strain-rate harden, such as Poly(methyl methacrylate) (PMMA),[19, 20] increasing near-surface hardness and modulus has been attributed to a strain-rate effect. In a load-controlled (constant velocity) indentation the strain rate will decrease with increasing indentation depth, which is thought responsible for

the apparent decrease in hardness with depth.[20] On PET, however, which unlike PMMA does not strain-rate harden, the explanation must be more complex.

Several factors can affect whether the normal relationship[17,18] between load and depth during an indentation ($P=a\,h^n$, $n=2$) holds. Deviations from this (i.e. $n<2$) can occur when (i) there is strain rate hardening, (ii) there are viscoelastic effects, (iii) the mechanical properties (hardness and modulus) vary with depth due to a changing crystallinity profile. It is clear that viscoelastic effects are important for PET since n is always less than 2 in our tests. Viscoelastic effects can be also be inferred from the observed variation in the indentation exponent, n, with loading rate.

A similar result[7] that values of n, determined by a different procedure, tended to decrease nearer the surface, and that this tendency was increased on drawn PET films. It has previously been suggested that PET films are more crystalline in the near-surface region than in the bulk[21], possibly due to orientation-induced crystallization. In view of this, the conclusion that the industrial treatment processes applied on PET before its commercial disposal [stretching (drawing) the films] has a greater effect of the topmost layers seems reasonable, although clearly, care must be taken in interpreting the near-surface indentation response of viscoelastic-plastic materials.

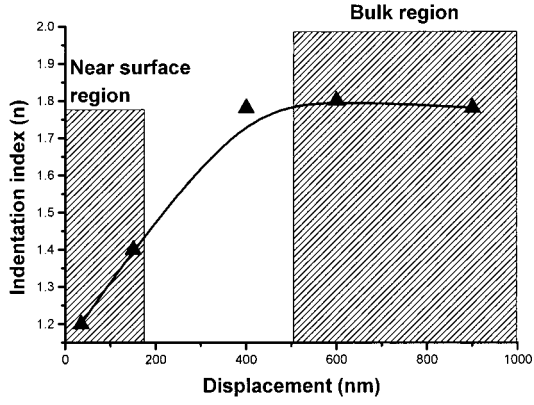

Figure 6. Indentation index (n) vs. Displacement of the indenter into the PET membrane.

Conclusions

Results from the nanomechanical characterization of the PET membranes are consistent with the resulting composition and geometrical structure of PET membranes based on SE data analysis and support their interrelation. Nanoindentation testing and SE measurements and analyses have revealed significant differences in the nanomechanical properties and composition of the surface/near surface region of the PET membranes, which exhibits higher hardness and elastic modulus, presumably due to its higher crystallinity in comparison with those of bulk PET.

Acknowledgements

This work was supported by the EU GROWTH Project – TransMach (Contract No: G1RD-CT-2000-000334) and partly by the Greek General Secretariat for Research and Technology, BILATERAL COOPERATION IN SCIENCE & TECHNOLOGY (GREECE-GERMANY) Project No. 2000ΣΕ01330005.

[1] Y. Dirix, H. Jagt, R. Hikmet, C. Bastiaansen, *J. Appl. Phys.* **1998**, *83 (6)*, 2927.
[2] M. Yanaka, B.M. Henry, A.P. Roberts, C.R.M. Grovenor, G.A.D. Briggs, A.P. Sutton, T. Miyamoto, Y. Tsukahara, N. Takeda, R.J. Chater, *Thin Solid Films* **2001**, *397*, 176.
[3] A.E. Tonelli, Polymer 43 (2002) 637.
[4] K. Forcht, A. Gombert, R. Joerger, M. Köhl, *Thin Solid Films* **1998**, *313-314*, 808.
[5] A. Flores, F.J. Balta Calleja, *Phil. Mag. A* **1998**, 78, 1283.
[6] F.J. Baltá Calleja and S. Fakirov. *Microhardness of Polymers*, Cambridge University Press, Cambridge, UK (2000).
[7] R.H. Ion, H.M. Pollock, C Roques-Carmes, *J. Mater. Sci.* **1990**, *25*, 1444.
[8] B.J. Briscoe, L. Fiori and E. Pelillo. *J Phys D* **1998**, *31*, 2395.
[9] B.D. Beake, G.J. Leggett, *Polymer* **2002**, *43*, 319.
[10] F. Benítez, E. Martínez, M. Galán, J. Serrat and J. Esteve. *Surf. Coat. Techn.* **2000**, *215*, 383.
[11] B.D. Beake, J.S.G. Ling and G.J. Leggett. *Polymer* **2000**, *41*, 2241.
[12] B.D. Beake, N.J. Brewer and G.J. Leggett. *Macromol Symp* **2001**, *167*, 101.
[13] W. C. Oliver and G. M. Pharr, *J. Mater. Res.* **1992**, *7*, 1564; S. Logothetidis and C. Charitidis, *Thin Solid Films* **1999**, *353*, 208.
[14] G.E. Jelison and F.A. Modine, *Appl. Phys. Lett.* **1996**, *69*, 371.
[15] S. Logothetidis, M. Gioti, C.Gravalidis, *Synthetic Metals* **2003**, *1-6*, 10358.
[16] Wu Yuguang et al., *Surf. and Coat. Technol.* **2001**, *148*, 221.
[17] S.V. Hainsworth, H.W. Chandler and T.F. Page. *J. Mater. Res.* **1996**, *11*, 1987.
[18] J. Malzender, G. de With and J.M.J. den Toonder. *J. Mater. Res.* **2000**, *15*, 1209.
[19] B.J. Briscoe, L. Fiori and E. Pelillo. *J. Phys. D* **1998**, *31*, 2395.
[20] S.A. Johnson. Nanoindentation and nanoscratch testing of organic coatings, UK Coatings Forum, London (2001).
[21] N.W. Hayes, G. Beamson, D.T. Clark, D.S.-L Law, R. Raval, *Surf. Interf. Anal.* **1996**, *24*, 723.